Topics in Catalysis (2020) 63:370–377
https://doi.org/10.1007/s11244-020-01258-3

ORIGINAL PAPER

The Effect of Co-feeding Methyl Acetate on the H-ZSM5 Catalysed Methanol-to-Hydrocarbons Reaction

A. Zachariou[1,2] · A. P. Hawkins[1,2] · P. Collier[3] · R. F. Howe[4] · S. F. Parker[1,5] · D. Lennon[1]

Published online: 3 April 2020

Abstract
The reactivity of methanol and methyl acetate mixtures over a HZSM-5 catalyst is studied over a period of 6 h at 350 °C, with small molecular weight olefins and aromatic compounds observed as reaction products. Post-reaction analysis of the catalyst shows the coke content to increase with methyl acetate content. Vibrational spectra (DRIFTS and inelastic neutron scattering, INS) indicate the major hydrocarbon species present in the coked catalysts to be methylated aromatic molecules, with INS spectra indicating a greater degree of methylation in the catalysts used with higher methyl acetate content. The greater extent of deactivation at higher methyl acetate concentrations is tentatively attributed to a diminishment of water in the zeolite cavity, which would otherwise facilitate re-generation of the active sites.

Keywords HZSM-5 · Methanol-to-hydrocarbons reaction · Methyl acetate · Inelastic neutron scattering

1 Introduction

The methanol-to-hydrocarbons reaction (MTH) provides a catalytic route where methanol, a relatively cheap feedstock, can be turned into more valuable and industrially relevant products. The MTH reaction uses an acidic zeolite catalyst, commonly ZSM-5, which can produce light olefins and a range of methylated aromatics [1]. The catalyst at steady-state is thought to operate via a 'hydrocarbon pool' (HCP) mechanism. The HCP mechanism is an autocatalytic cycle that describes how the catalyst functions after the first hydrocarbons have formed [2, 3]. However, the mechanism of formation of the first carbon–carbon bonds is still elusive, with many different proposals in the literature [4].

Understanding how the first C–C bonds are created may help optimisation of catalyst composition in order to both maximise efficiency but also tune selectivity. One recent proposal independently reported by the groups of Lercher [5] and Weckhuysen [6] is that carbon–carbon bonds are created via methyl acetate (MeOAc) as the first intermediate. [5, 6]. Formation of MeOAc from methanol or dimethylether (DME) requires the feedstock to undergo a carbonylation reaction, which forms surface acetate groups. The carbonylation reaction also requires a source of CO, which Lercher et al. suggest may result from dehydrogenation of methanol [5]. Methanol and DME carbonylation to form MeOAc has been reported mainly with a mordenite acid zeolite catalyst, although good selectivity towards MeOAc at relatively lower temperatures has also been observed with HZSM-5 [7, 8]. CO has also been observed as part of the initial stages of the MTH reaction, both on ZSM-5 and on SAPO-34 [9, 10]. In studies where the carbonylation reaction was the main focus, it has been reported that water causes the carbonylation rate to decrease due to competitive adsorption with the CO, since methanol is dehydrated to form DME and water, the carbonylation step is expected to be the rate limiting step of the MTH reaction [7, 11].

In this study we have explored the reactivity of methanol–MeOAc mixtures over an HZSM-5 catalyst at

✉ D. Lennon
David.Lennon@glasgow.ac.uk

1 School of Chemistry, University of Glasgow, Joseph Black Building, Glasgow G12 8QQ, UK

2 UK Catalysis Hub, Research Complex at Harwell, STFC Rutherford Appleton Laboratory, Chilton, Oxon OX11 0FA, UK

3 Johnson Matthey Technology Centre, Blounts Court, Sonning Common, Reading RG4 9NH, UK

4 Department of Chemistry, University of Aberdeen, Aberdeen AB24 3UE, UK

5 ISIS Facility, STFC Rutherford Appleton Laboratory, Chilton, Oxon OX11 0QX, UK

temperatures representative of that employed in MTH chemistry. We particularly focus on the effects of MeOAc on the catalyst lifetime, employing inelastic neutron scattering spectroscopy (INS) to characterise the used catalysts. INS has considerable potential for investigating zeolite catalysts as it provides access to the vibrational spectra of used catalysts over a wide frequency range without obstruction from zeolite lattice modes [12]. We have recently reported the use of INS to study HZSM-5 catalysts used in the MTH reaction [13, 14] and the role of DME in the MTH reaction chemistry [15].

In the present work we examine the MTH reaction for a period of 6 h at 350 °C in the presence of different amounts of MeOAc. The reaction was monitored by in-line mass spectrometry whilst, additionally, liquid products were collected in a catch-pot and analysed by GC–MS. Post-reaction, the catalyst samples were analysed by INS, N_2 sorption experiments and temperature programmed oxidation (TPO).

2 Experimental

The HZSM-5 (Si:Al ratio = 30) zeolite used is a commercially available catalyst provided in powder form by Johnson Matthey plc. Catalyst characterisation has been reported elsewhere [13]. Residual HZSM-5 template (tetrapropyl ammonium bromide) was removed by heating the zeolite in air at 500 °C for 12 h prior to use.

2.1 Reaction Testing

The reactions were conducted using a reaction test facility located in the ISIS Neutron and Muon Source that is described in detail by Warringham et al. [16]. The fixed bed reactor is made of stainless steel with an internal diameter of 35 mm and length of 60 cm. 12 g of calcined HZSM-5 were loaded on the reactor and dried under a constant flow of He (150 ml min^{-1}, CK gas, > 99%) at 350 °C for 3 h. After the drying process, the reactor is kept at temperature and the reactant feed was introduced into the reactor at a rate of 1 $g_{reactant}\ g_{catalyst}^{-1}\ h^{-1}$. The reactant feed was a liquid mixture of methanol and methyl acetate (with molar percentages of 0% MeOAc, 10% MeOAc, 30% MeOAc, 60% MeOAc and 100% MeOAc) and all reactions were stopped after 6 h. The reactor was then flushed for 15 min with helium to remove any excess reactant feed present before being isolated and allowed to cool to ambient temperature.

2.2 Product Analysis

Gaseous products were analysed by in-line mass spectrometry (Hiden Analytical, HPR-20) connected to the exit line of the reactor via a differentially-pumped heated quartz capillary. A catch-pot placed downstream of the reactor was used to collect liquid products. They were analysed by off-line GC–MS (Agilent 7890A GC, 5975 MSD, DB-1MS capillary l: 60 m, ID 0.25 mm, t 0.25 μm). Initial oven temperature 40 °C held for 2 min, increased at a ramp rate of 10 °C min^{-1} to 150 °C and held for 3 min.

2.3 Post-reaction Catalyst Analysis

For the INS measurements all sample handling was conducted in an argon filled glove box (MBraun UniLab MB-20-G, $[H_2O] < 1$ ppm, $[O_2] < 1$ ppm). The reacted catalyst was removed from the reactor and transferred into aluminium INS flat cells sealed with indium wire. INS spectra were collected with the TOSCA instrument. TOSCA is an indirect geometry instrument with a spectral range of 25 to 4000 cm^{-1} but is optimal below 2000 cm^{-1}. Some of the reacted catalyst was kept for further analysis using diffuse reflectance infrared Fourier transform spectroscopy (DRIFTS), nitrogen adsorption and temperature programmed oxidation (TPO).

TPO experiments were conducted on the post-reacted ZSM-5 samples using a Hiden CatLab Microreactor integrated with a mass spectrometer and the coke weight percent was verified by thermogravimetric analysis (TGA) using the same procedure (TGA Q50, TA instruments). Approximately, 0.05 g of reacted catalyst was placed in a quartz reactor and dried at 300 °C until no water was detected in the mass spectrometer. The TPO was carried out under 20% O_2/He with increasing temperature from 40 to 800 °C at a heating rate of 10 °C min^{-1}. TGA was completed in the same way, however, air was used instead of the O_2/He mixture.

Surface area analysis was completed using a Quantachrome Quadrasorb EVO/Si gas adsorption instrument. 0.15 g of sample was placed in a 9 mm quartz sample tube and was degassed at < 20 mTorr at 200 °C for 20 h. The weight of the sample was recorded before being mounted on the Quadrasorb instrument. The Brunauer–Emmett–Teller (BET) equation was used to calculate the surface area in the pressure range P/P_0 of 0.02–0.04. The micropore volume was calculated from the t-plot curve using the thickness range between 5 and 6.9 Å. Adsorption isotherm analysis was completed using the QuadraWin software.

DRIFTS spectra were collected using an Agilent Carey 680 FTIR spectrometer equipped with a Harrick Praying Mantis accessory. Catalyst samples were loaded under argon into the Harrick Praying Mantis high temperature in situ cell fitted with ZnSe windows. It was then heated in flowing nitrogen (50 mL min^{-1}) at a ramp rate of 10 °C min^{-1} to 350 °C and held at 350 °C for 30 min. Spectra were collected with 64 scans at 4 cm^{-1} resolution using a liquid nitrogen cooled MCT detector.

3 Results

3.1 Reaction Monitoring

Figure 1 shows the product profiles versus time on stream for (a) methanol alone, (b) methanol:MeOAc 7:3, (c) methanol:MeOAc 4:6 and (d) MeOAc alone. The mass spectrometric analysis is complicated by the contributions from fragmentation of other species but, nonetheless, a number of trends can be identified. For methanol alone, the formation of ethene, propene and aromatic products remains effectively constant over the 6 h run time. Although there is some increase in the amount of unreacted methanol and DME over this time period, the overall conversion of methanol remains high (> 90%). Figure 2 plots the methanol and MeOAc conversions versus time for the different reactant compositions tested (conversions were calculated from comparison with mass spectral peak intensities measured at time = 0 on bypassing the reactor). Figure 1b shows the addition of 30% MeOAc leads to a proportionally greater degree of aromatic products, whilst Fig. 2 shows both MeOH and MeOAc conversions to remain high. Over the range 0–30% MeOAc content, Fig. 2a shows methanol conversion to be slightly improved in increasing MeOAc; for example at 5 h T-o-S 10% and 30% MeOAc return X_{MeOH} values of 99.0% and 99.9% respectively, compared to a value of 98.0% for a pure methanol feed. These small shifts in methanol conversion may reflect changes in the formation of the hydrocarbon pool on increasing presence of the ester.

At 60% MeOAc Fig. 2 shows a noticeable deactivation to occur. The methanol conversion falls steadily throughout the run and, although aromatic production continues (Fig. 1c), the apparent continued production of ethene and propene is largely due to the contributions to m/z = 42 and 27 from fragmentation of unreacted MeOAc. For a pure MeOAc feedstream, Fig. 1d shows the aromatic signal to steadily

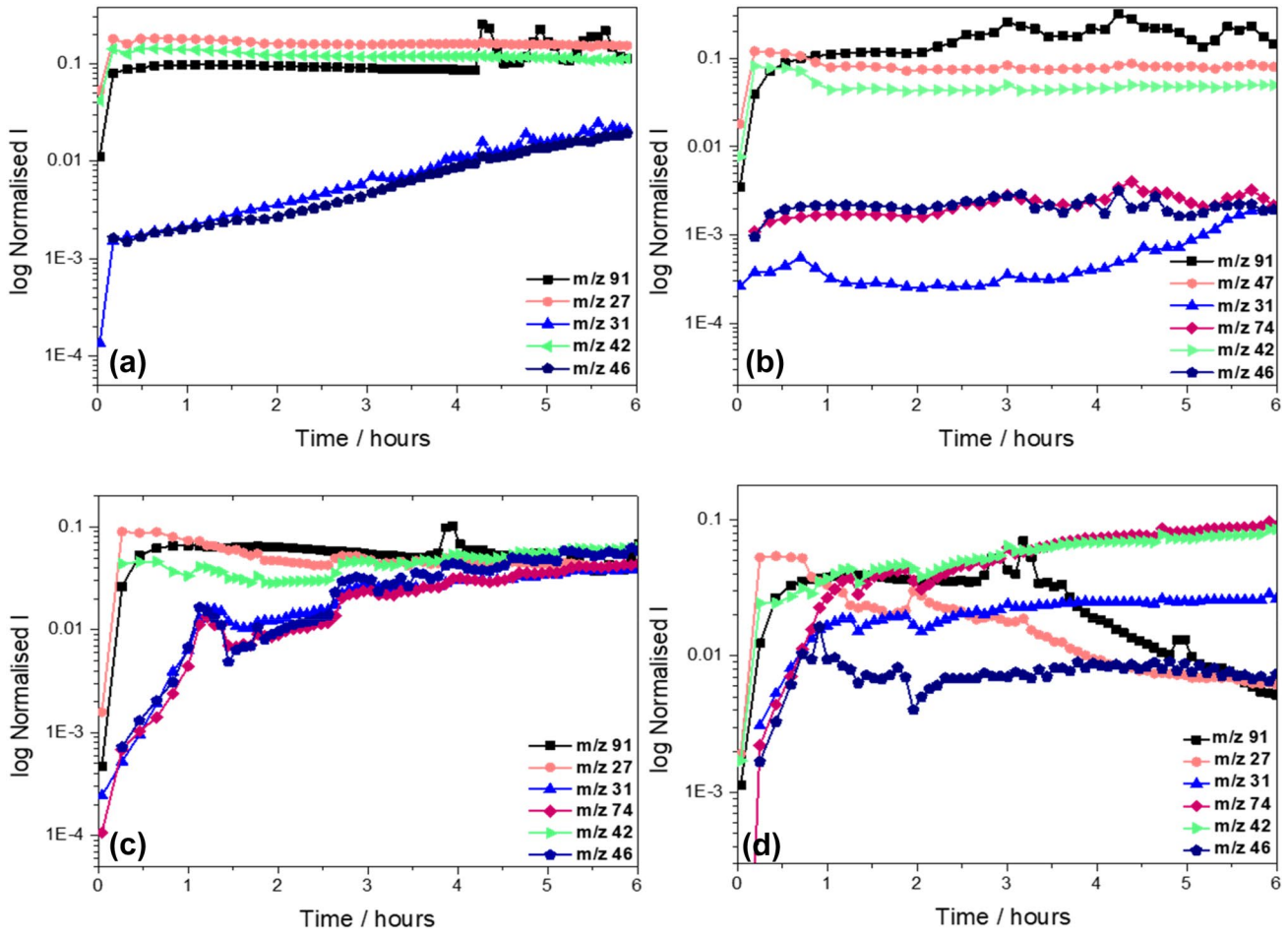

Fig. 1 Mass spectral analysis of reactor exit gases during MeOH/MeOAc conversion at 350 °C. **a** 0% MeOAc, **b** 30% MeOAc, **c** 60% MeOAc and **d** 100% MeOAc. m/z 91 (—■—) signifies the tropylium ion indicating aromatics. m/z 74 (—◆—) signifies methyl acetate, m/z 46 (—●—) signifies DME, m/z 42 (—▶—) signifies propene, m/z 31 (—▲—) signifies methanol and m/z 27 (—●—) signifies ethene

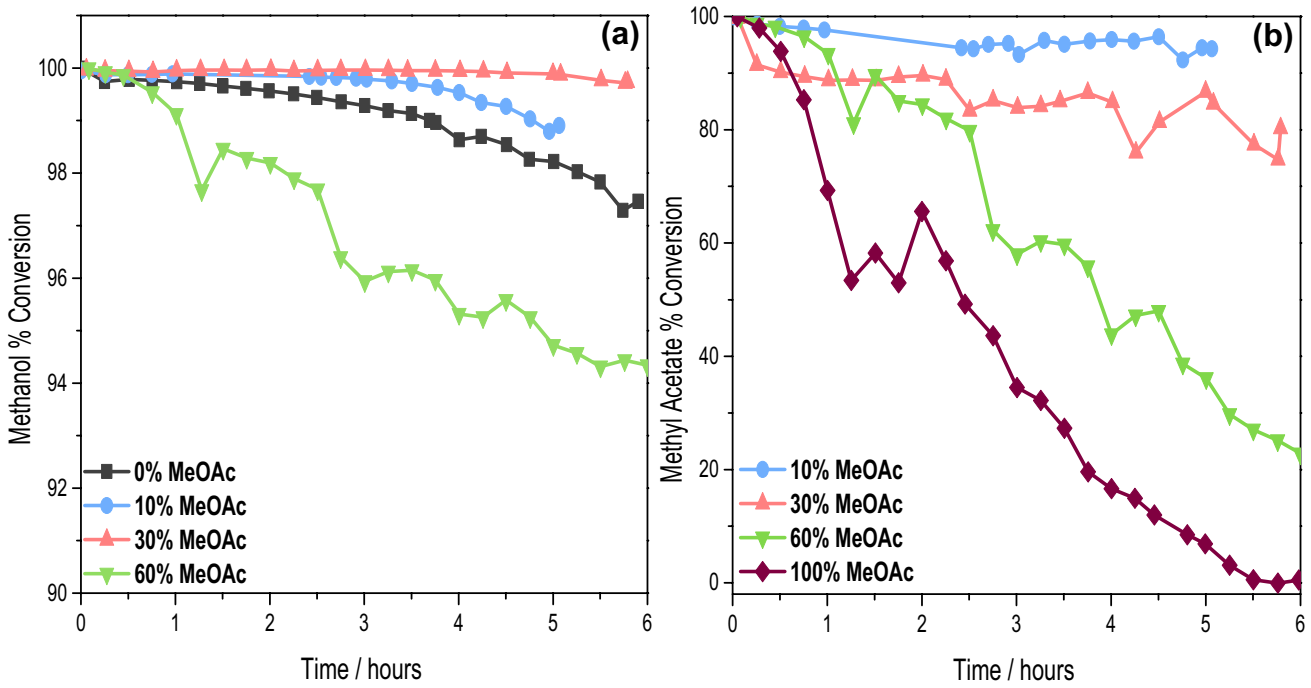

Fig. 2 Methanol (**a**) and methyl acetate (**b**) percentage conversion versus time on stream at 350 °C

decline after ~ 3 h time-on-stream. There is also a significant increase in the methanol signal, suggesting that hydrolysis of MeOAc may be occurring.

Figure 3 shows GC–MS analysis of the liquid products retained in the reactor catchpot (total product after 6 h on stream). For pure MeOAc as the reactant, acetic acid is the major liquid product. In all of the reactions, the hydrocarbon products comprise a mixture of xylenes, tri-methylbenzenes, tetra-methylbenzenes and substituted naphthalenes. These products are still present but at much lower levels when pure MeOAc was the reactant.

The conversion of MeOAc over SAPO-34 catalysts is reported to give an initial product distribution similar to that formed from methanol, although the production of alkenes falls after only 10 min on stream at 400 °C [17]. We are not aware of any comparable study of MeOAc conversion over

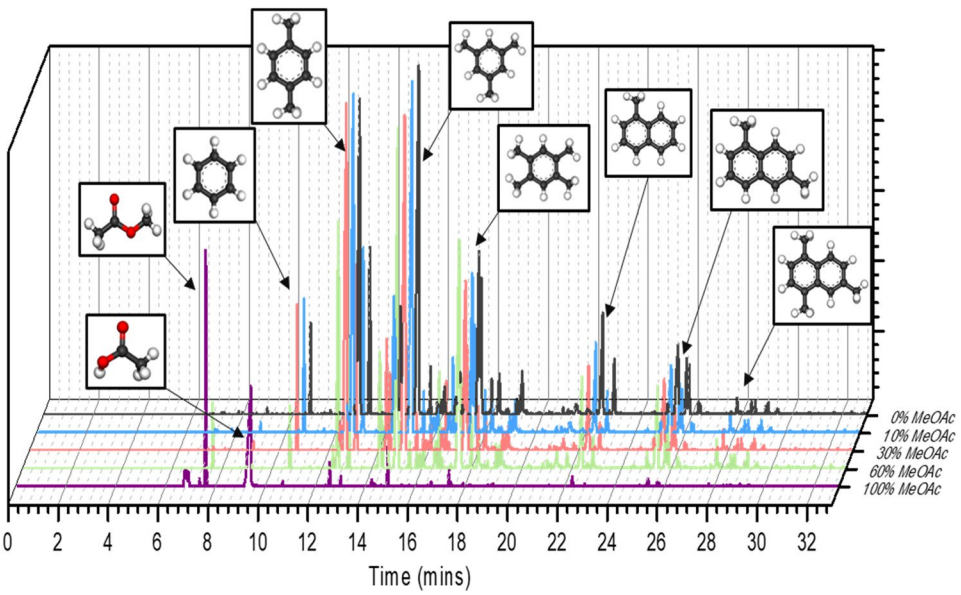

Fig. 3 Catch-pot analysis via GC–MS of liquid products accumulated during 6 h on stream at 350 °C

Table 1 Coke content and nitrogen sorption data for the used catalysts

Reaction feed	Coke content (wt%)	BET surface area ($m^2\ g^{-1}$)	Micropore volume ($cm^3\ g^{-1}$)
Fresh ZSM-5 [15]	0	387	0.148
0% MeOAc	2.53	302	0.112
10% MeOAc	2.81	327	0.121
30% MeOAc	7.55	155	0.054
60% MeOAc	9.33	40.6	0.009
100% MeOAc	9.76	22.1	0.003

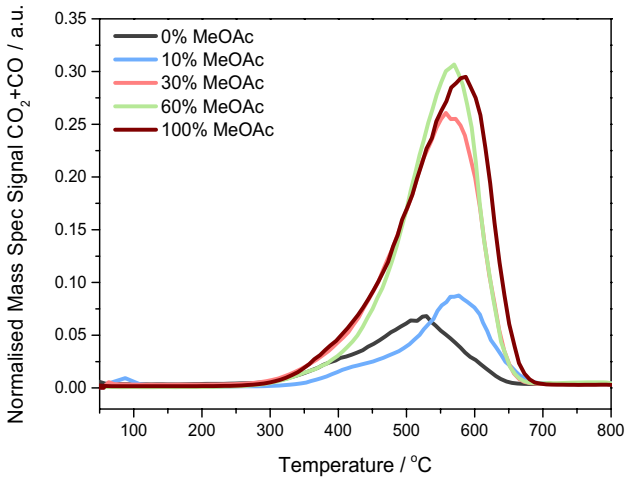

Fig. 4 TPO profiles of the reacted ZSM-5 zeolites

HZSM-5, although we note that coupling of CO and methanol over HZSM-5 is reported to form aromatic products, presumably via MeOAc [18]. The results presented above suggest that the major role of MeOAc is to promote catalyst deactivation. Accordingly, we examined the used catalysts from the above reactions in more detail.

3.2 Post-reaction Catalyst Characterisation

Consistent with the suggested role of MeOAc in promoting catalyst deactivation, the coke content of the used catalysts increased with increasing MeOAc content of the reaction feed, as shown in Table 1. It is noted that this systematic trend contrasts with the small and somewhat anomalous methanol conversion trends observed in Fig. 2a. There is also a corresponding loss of surface area, principally micropore volume, which correlates with the increasing coke content.

These data are consistent with earlier reports that initial coke formation in methanol conversion over HZSM-5 occurs within the micropores of the zeolites [19]. Temperature-programmed oxidation measurements reveal that addition of MeOAc to the reaction feed causes some change in the nature of the coke species. (Fig. 4).

There is a significant shift to higher temperature in the peak maximum in the TPO profile of the used catalysts when MeOAc is added to the feed, from ~ 520 to 580 °C. The shift being observed even when 10% MeOAc is added to the methanol feed. This suggests that in the presence of MeOAc the coke deposits have a lower H:C ratio than that formed from methanol alone, although there is no evidence for the presence of "hard" or graphitic coke [20] even with a pure MeOAc feed at 350 °C. The peak shift is consistent with an increased presence of aromatics when methyl acetate is added to the methanol feed.

Figure 5 shows DRIFTS spectra of the used catalysts in the 4000–2200 cm^{-1} region, in all cases recorded at 350 °C in flowing helium. The blank zeolite dehydrated at 350 °C shows two characteristic ν(OH) bands at 3735 and 3596 cm^{-1} assigned respectively to SiOH groups on the external surface or in defects and to Si(OH)Al Brønsted acid sites [21, 22]. An additional weak shoulder at 3650 cm^{-1} is due to extra-framework AlOH groups [23, 24]. The used catalysts all show attenuation of the Brønsted acid band, which becomes more attenuated as the MeOAc content of the feed increases. At higher MeOAc concentrations the silanol and extra-framework AlOH bands are also attenuated. The attenuation of the Brønsted acid sites was seen previously in catalysts used for methanol conversion at 350 °C for 3 days [13], consistent with coke formation at the acid sites. Attenuation of the silanol and extra-framework AlOH sites is associated specifically with the presence of MeOAc.

In the ν(CH) region the four bands appearing at 3121, 2971, 2926 and 2869 cm^{-1} closely resemble those reported by Suwardiyanto et al. [13] and assigned to methylated aromatic hydrocarbon species trapped in the zeolite pores. The intensities of these bands increase with MeOAc content of the feed, as does the coke content, but from this region of the infrared spectrum we cannot identify any differences in the nature of the coke species formed from methanol versus MeOAc. Accordingly, we turned to INS spectroscopy to observe the lower frequency vibrational spectra.

3.3 Inelastic Neutron Scattering

Figure 6 shows INS spectra of the blank zeolite, the zeolite containing MeOAc adsorbed at room temperature, and a sample of pure MeOAc. The spectra are normalised with respect to the weight of the sample. The dosed MeOAc on ZSM-5 shows that the MeOAc remains intact on the ZSM-5 with all the major peaks distinguishable. The peaks become broadened and less intense which could be attributed to the confinement effects of the MeOAc inside the zeolite structure. The blank ZSM-5 spectrum is shown as a reference, showing that the zeolite contribution to the spectra is

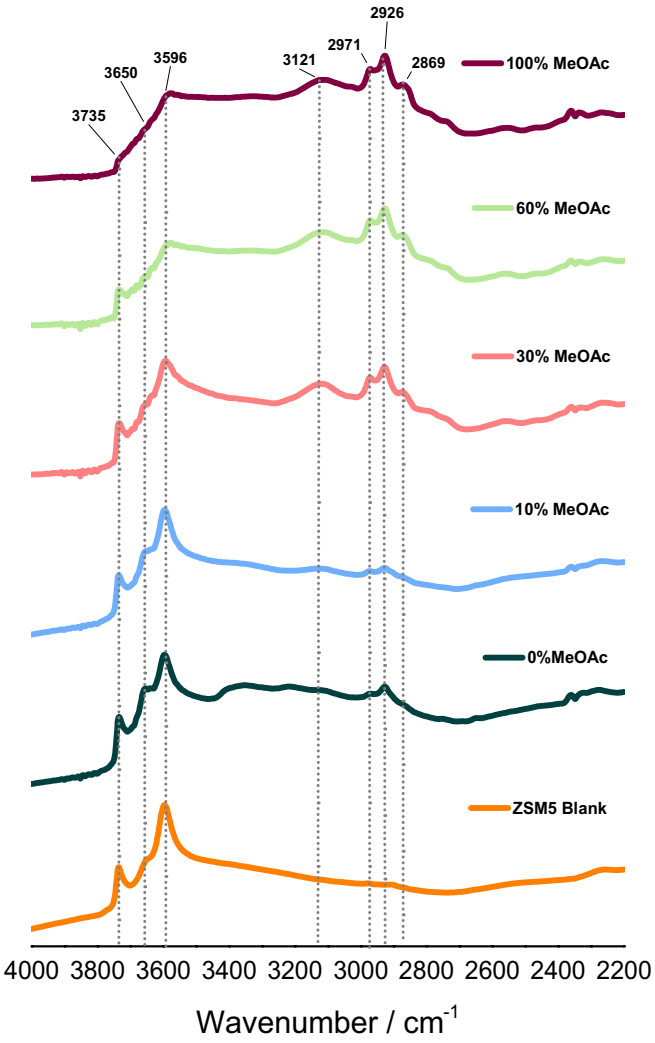

Fig. 5 DRIFTS Spectra of the reacted samples. Spectra were normalised with respect to the zeolite framework peaks at 1864 cm^{-1} and 1972 cm^{-1}

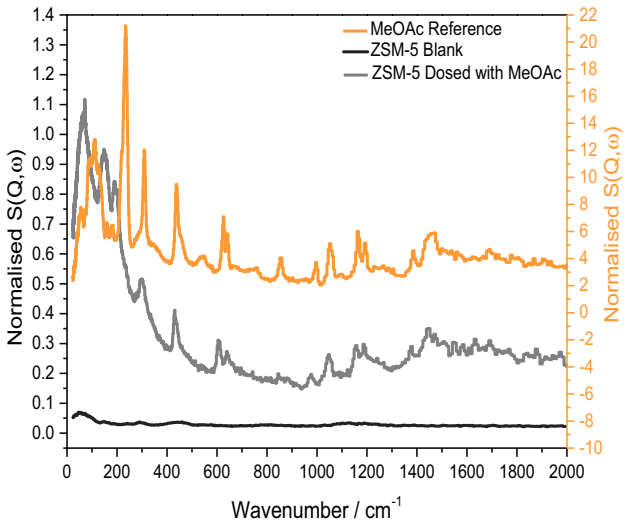

Fig. 6 INS spectra of the blank zeolite (black), methyl acetate (orange) and methyl acetate exposed to ZSM-5 at ambient temperature (grey)

minimal (and emphasising the advantage of INS for studying this region of the spectrum).

Figure 7 shows spectra recorded over the same frequency range for the used catalyst samples. As with the infrared spectra in Fig. 5, the intensities of the bands due to hydrocarbon coke species increase with increasing MeOAc content in the feed. This trend additionally reflects that observed for retained coke content (Table 1). No evidence of features attributable to surface bound methyl acetate entities is apparent in either the IR or INS spectra.

Interestingly, the spectra measured from catalysts exposed to 30% or more MeOAc resemble those previously reported for HZSM-5 zeolite catalysts reacted with dimethylether at 350 °C [15] and importantly have no correspondence to the spectrum of adsorbed MeOAc (Fig. 6). For example, the doublet at 1370 and 1456 cm^{-1} in Fig. 7 is respectively assigned to CH_3 symmetric and asymmetric bending modes of methyl groups attached to aromatic rings and both features are present in all of the spectra except that of the 0% MeOAc catalyst. A band at 1186 cm^{-1} is present

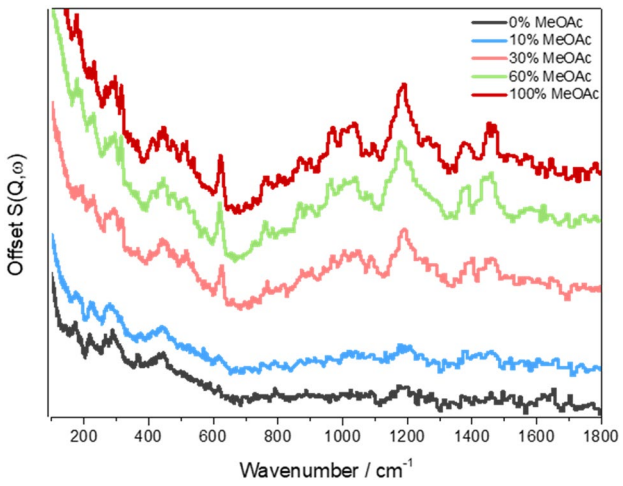

Fig. 7 INS spectra of ZSM-5 samples reacted at 350 °C for 6 h with a feed of 0% MeOAc, 10% MeOAc, 30% MeOAc, 60% MeOAc and 100% MeOAc

in all spectra, and appears to grow together with the 1370, 1456 cm^{-1} doublet, suggesting it is associated with the same species. Likewise, the lower frequency bands are similar to those seen with dimethylether as the reactant [15]. Some differences in relative intensity are noted: bands between 800 and 1000 cm^{-1} are assigned to aromatic CH out-of-plane bending modes which are less intense in Fig. 7 relative to the 1033 cm^{-1} band due to CH_3 rocking modes compared with the spectra of the dimethylether catalysts [15]. We attribute these differences to a greater degree of methylation of the aromatic rings in the presence of MeOAc. Highly methylated aromatics have been linked with ZSM-5 deactivation [19, 25], which could explain why the increase in MeOAc has also nudged the catalyst in to a deactivation stage earlier than is seen with either methanol or DME. This enhanced extent of methylation in the adsorbed aromatic hydrocarbons appears to be the only significant difference in the INS spectra between the coke deposits formed in the presence and absence of MeOAc.

4 Discussion

Methyl acetate has been included in the methanol feedstream and its role in MTH chemistry over HZSM-5 considered. Methyl acetate additions over the range 10–100% are seen to modify the product distribution of low molecular weight olefins plus aromatic compounds and perturb methanol conversion. The ester appears to accelerate catalyst deactivation by enhancing the formation of methylated aromatic coke compounds that block active sites within the zeolite. Müller et al. [26] have suggested that initial coke formation in ZSM-5 is enhanced by the presence of oxygenated compounds, but the vibrational spectroscopic data show no evidence for the presence of anything other than methylated aromatics in the used catalysts studied here, and the TPO data show no sign of the Type I coke observed in reference [26]. One possible origin for the deactivation trends observed could be that the presence of methyl acetate in the feedstream leads to a constrained supply of water molecules in the reaction zone (formed as a product in the dimerization of methanol to produce dimethyl ether), which would otherwise facilitate re-generation of the active sites (Brønsted acid sites) [15].

Acknowledgements Johnson Matthey plc and the EPSRC are thanked for postgraduate student support (A.P.H., A.Z.) via the Industrial CASE scheme (EP/P510506/1). Johnson Matthey plc is additionally thanked for provision of the ZSM-5 catalyst. The Science and Technology Facilities Council is thanked for the provision of neutron beam time (RB1820116, https://doi.org/10.5286/isis.e.97999822). The resources and support provided by the UK Catalysis Hub via Membership of the UK Catalysis Hub Consortium and funded by EPSRC (Grants EP/K014706/1, EP/K014668/1, EP/ K014854/1, EP/K014714/1, and EP/M013219/1) are gratefully acknowledged.

Data Availability The datasets generated during and/or analysed during the current study are available from the corresponding author on reasonable request.

Compliance with Ethical Standards

Conflicts of interest The authors have no conflicts of interest.

Research Invloving Human and/or Animal Rights There were no human or animal subjects involved in this research.

References

1. Chang CD (1983) Hydrocarbons from methanol. Catal Rev 25:1–118
2. Olsbye U, Svelle S, Lillerud KP et al (2015) The formation and degradation of active species during methanol conversion over protonated zeotype catalysts. Chem Soc Rev 44:7155–7176
3. Hemelsoet K, Van der Mynsbrugge J, De Wispelaere K et al (2013) Unraveling the reaction mechanisms governing methanol-to-olefins catalysis by theory and experiment. ChemPhysChem 14:1526–1545

4. Yarulina I, Chowdhury AD, Meirer F et al (2018) Recent trends and fundamental insights in the methanol-to-hydrocarbons process. Nat Catal 1:398–411
5. Liu Y, Müller S, Berger D et al (2016) Catalytic mechanisms formation mechanism of the first carbon–carbon bond and the first olefin in the methanol conversion into hydrocarbons. Angew Chem Int Ed 55:5723–5726
6. Chowdhury AD, Houben K, Whiting GT et al (2016) Initial carbon–carbon bond formation during the early stages of the methanol-to-olefin process proven by zeolite-trapped acetate and methyl acetate. Angew Chem Int Ed 55:15840–15845
7. Cheung P, Bhan A, Sunley GJ, Iglesia E (2006) Selective carbonylation of dimethyl ether to methyl acetate catalyzed by acidic zeolites. Angew Chem Int Ed 45:1617–1620
8. Wang S, Li S, Zhang L et al (2018) Mechanistic insights into the catalytic role of various acid sites on ZSM-5 zeolite in the carbonylation of methanol and dimethyl ether †. Catal Sci Technol 8:3193
9. Haas A, Hauber C, Kirchmann M (2019) Time-resolved product analysis of dimethyl ether-to-olefins conversion on SAPO-34. https://doi.org/10.1021/acscatal.9b00765
10. Anderson MW, Klinowski J (1989) Direct observation of shape selectivity in zeolite ZSM-5 by magic-angle-spinning NMR. Nature 339:200–203
11. Jiang Y, Hunger M, Wang W (2006) On the reactivity of surface methoxy species in acidic zeolites. https://doi.org/10.1021/JA061018Y
12. Parker SF, Lennon D, Albers PW (2011) Vibrational spectroscopy with neutrons: a review of new directions. Appl Spectrosc 65:1325–1341
13. Suwardiyanto, Howe RF, Catlow RCA et al (2017) An assessment of hydrocarbon species in the methanol-to-hydrocarbon reaction over a ZSM-5 catalyst. Faraday Discuss 197:447
14. Howe RF, McGregor J, Parker SF et al (2016) Application of inelastic neutron scattering to the methanol-to-gasoline reaction over a ZSM-5 catalyst. Catal Lett 146:1242–1248
15. Zachariou A, Hawkins A, Lennon D et al (2019) Investigation of ZSM-5 catalysts for dimethylether conversion using inelastic neutron scattering. Appl Catal A 569:1–7
16. Warringham R, Bellaire D, Parker SF et al (2014) Sample environment issues relevant to the acquisition of inelastic neutron scattering measurements of heterogeneous catalyst samples. J Phys Conf Ser 554:012005
17. Chowdhury AD, Paioni AL, Houben K et al (2018) Bridging the gap between the direct and hydrocarbon pool mechanisms of the methanol-to-hydrocarbons process. Angew Chem Int Ed 57:8095–8099
18. Chen Z, Ni Y, Zhi Y et al (2018) Coupling of methanol and carbon monoxide over H-ZSM-5 to form aromatics. Angew Chem Int Ed 57:12549–12553
19. Bibby DM, Howe RF, Mclellan GD (1992) Coke formation in high-silica zeolites. Appl Catal A 93:1–34
20. Choudhary VR, Devadas P, Sansare SD, Guisnet M (1997) Temperature programmed oxidation of coked H-gallosilicate (MFI) propane aromatization catalyst: influence of catalyst composition and pretreatment parameters. J Catal 166:236–243
21. Jacobs PA, Von Ballmoos R (1982) Framework hydroxyl groups of H-ZSM-5 zeolites. J Phys Chem 86:3050–3052
22. Vedrine JC, Auroux A, Coudurier G (1984) Combined physical techniques in the characterization of zeolite ZSM-5 and ZSM-11 acidity and basicity. In: ACS symposium series, pp 254–273
23. Kubelková L, Nováková J, Nedomová K (1990) Reactivity of surface species on zeolites in methanol conversion. J Catal 124:441–450
24. Campbell SM, Bibby DM, Coddington JM et al (1996) Dealumination of HZSM-5 zeolites: I. Calcination and hydrothermal treatment. J Catal 161:338–349
25. Rojo-Gama D, Nielsen M, Wragg DS et al (2017) A straightforward descriptor for the deactivation of zeolite catalyst H-ZSM-5. ACS Catal 7:8235–8246
26. Müller S, Liu Y, Vishnuvarthan M et al (2015) Coke formation and deactivation pathways on H-ZSM-5 in the conversion of methanol to olefins. J Catal 325:48–59